

Resource Allocation in GMD and SVD-based MIMO System

Andreas Ahrens¹, Francisco Cano-Broncano² and César Benavente-Peces²

¹*Hochschule Wismar, University of Technology, Business and Design, Philipp-Müller-Straße 14, 23966 Wismar, Germany*

²*Universidad Politécnica de Madrid, Ctra. Valencia. km. 7, 28031 Madrid, Spain*

Keywords: Multiple-input Multiple-output System, Singular-value Decomposition, Geometric Mean Decomposition, Bit Allocation, Power Allocation, Antennas Correlation, Wireless Transmission, Tomlinson-harashima Precoding.

Abstract: Singular-value decomposition (SVD)-based multiple-input multiple output (MIMO) systems, where the whole MIMO channel is decomposed into a number of unequally weighted single-input single-output (SISO) channels, have attracted a lot of attention in the wireless community. The unequal weighting of the SISO channels has led to intensive research on bit- and power allocation even in MIMO channel situation with poor scattering conditions identified as the antennas correlation effect. In this situation, the unequal weighting of the SISO channels becomes even much stronger. In comparison to the SVD-assisted MIMO transmission, geometric mean decomposition (GMD)-based MIMO systems are able to compensate the drawback of weighted SISO channels when using SVD, where the decomposition result is nearly independent of the antennas correlation effect. The remaining interferences after the GMD-based signal processing can be easily removed by using dirty paper precoding as demonstrated in this work. Our results show that GMD-based MIMO transmission has the potential to significantly simplify the bit and power loading processes and outperforms the SVD-based MIMO transmission as long as the same QAM-constellation size is used on all equally-weighted SISO channels.

1 INTRODUCTION

The strategy of placing multiple antennas at the transmitter and receiver sides, well-known as multiple-input multiple-output (MIMO) system, improves the performance of wireless systems by the use of the spatial characteristics of the channel (Zheng, 2003; Yang et al., 2011). MIMO systems have become the subject of intensive research over the past 20 years as MIMO is able to support higher data rates and shows a higher reliability than single-input single-output (SISO) systems (Jiang et al., 2008).

Singular-value decomposition (SVD) is well-established in MIMO signal processing where the whole MIMO channel is transferred into a number of weighted SISO channels. The unequal weighting of the SISO channels has led to intensive research to reduce the complexity of the required bit- and power-allocation techniques (Zanella and Chiani, 2012; Cano-Broncano et al., 2014) in rich and poor scattering conditions.

However, due to poor scattering conditions the unequal weighting of the SISO channels is strongly affected by the antennas correlation effect (Benavente-Peces et al., 2013; Chiani et al., 2003; Abdi and

Kaveh, 2002; Loyka and Tsoulos, 2002; Shiu et al., 1998), which makes the process of bit- and power-allocation more challenging.

The geometric mean decomposition (GMD) is a signal processing technique which decomposes the MIMO channel matrix in a different way (Jiang et al., 2005). Compared to the SVD-assisted MIMO transmission, GMD-based MIMO systems are able to compensate the drawback of weighted SISO channel when using SVD independently of the antennas correlation effect. By using the GMD, the whole MIMO system can be decomposed into a number of equally-weighted SISO channels, which significantly simplifies the process of bit- and power loading as long as the same QAM constellation sizes are used on all SISO channels. The remaining inter-antennas interferences as a result of the GMD-based signal processing can be easily removed by using dirty paper precoding, as demonstrated in this work.

The novelty of our contribution is that we demonstrate the benefits of amalgamating a suitable choice of activated MIMO layers and number of bits per sub-carrier along with the appropriate allocation of the transmit power under the constraint of a given fixed

data throughput. Here, optimal and suboptimal bit- and power-loading in both SVD- and GMD-based MIMO transmission systems with and without antenna correlation are elaborated. Assuming a fixed data rate, which is required in many applications (e.g., real time video applications), a two stage optimization process is proposed. Firstly, the allocation of bits to the number of SISO channels is optimized and secondly, the allocation of the available total transmit power is studied when minimizing the overall bit-error rate (BER) at a fixed data rate. Whereas optimal power allocation techniques are highly complex, suboptimal solutions offer a good compromise between complexity and performance lost compared with optimal solutions. Our results show that GMD-based MIMO transmission has the potential to significantly simplify the process of bit and power loading both in correlated and uncorrelated MIMO systems and outperforms SVD-based MIMO transmission as long as the same QAM-constellation size is used on all equally weighted SISO channels.

The remaining part of this paper is structured as follows: Section 2 introduces the MIMO system model and the signal processing techniques used in this work. In section 3 the well-know quality criteria is briefly reviewed and applied to our problem. The proposed resource allocation solutions are discussed in section 4, while the associated performance results are presented and interpreted in section 5. Finally, section 6 provides some concluding remarks.

2 MIMO SYSTEM MODEL

A frequency non-selective MIMO communication link with n_T antennas in transmission and n_R in reception can be described as

$$\mathbf{u} = \mathbf{H} \cdot \mathbf{c} + \mathbf{n} , \quad (1)$$

where \mathbf{u} corresponds to the $(n_R \times 1)$ received data vector, \mathbf{H} is the $(n_R \times n_T)$ channel matrix, \mathbf{c} is the $(n_T \times 1)$ transmitted data vector and \mathbf{n} is the $(n_R \times 1)$ Additive White Gaussian Noise (AWGN) vector. Furthermore, it is assumed that the coefficients of the channel matrix \mathbf{H} are independent and identically Rayleigh distributed with equal variance and that the number of transmit antennas equals the number of receive antennas $n_T = n_R$.

In MIMO systems, inter-antennas interferences appear due to the increased number of antennas and the consequent multipath signals. These interferences are described by the off-diagonal elements of the channel matrix \mathbf{H} . In order to avoid the inter-antenna interferences, appropriate signal processing

techniques are required. The Singular Value Decomposition (SVD) is used to transform the MIMO channel into independent layers. Given the channel matrix \mathbf{H} , the application of the SVD to \mathbf{H} allows expressing it as $\mathbf{H} = \mathbf{S} \cdot \mathbf{V} \cdot \mathbf{D}^H$, where the $(n_R \times n_R)$ matrix \mathbf{S} and the $(n_T \times n_T)$ matrix \mathbf{D}^H are unitary matrices, and \mathbf{V} is a real-valued diagonal matrix containing the positive square roots of the eigenvalues of the matrix $\mathbf{H}^H \mathbf{H}$ sorted in descending order, and $(\cdot)^H$ denotes the Hermitian transpose. Assuming perfect channel state information (PCSI) is available at both the transmit and receive sides, the application of pre- and post-processing decomposes the MIMO channel into multiple independent SISO layers with different gains given by the singular values in \mathbf{V} , consequently, the overall transmission relationship results in

$$\mathbf{y} = \mathbf{S}^H \cdot \mathbf{u} = \mathbf{S}^H (\mathbf{H} \cdot \mathbf{c} + \mathbf{n}) = \mathbf{S}^H (\mathbf{H} \cdot \mathbf{D} \cdot \mathbf{x} + \mathbf{n}) \quad (2)$$

which leads to

$$\mathbf{y} = \mathbf{V} \cdot \mathbf{x} + \mathbf{w} , \quad (3)$$

where \mathbf{x} is the $(n_T \times 1)$ pre-processed transmit data vector, \mathbf{y} is the $(n_R \times 1)$ post-processed receive data vector and the $(n_R \times 1)$ post-processed noise vector is given by $\mathbf{w} = \mathbf{S}^H \cdot \mathbf{n}$. The number of independent SISO layers is limited by $\min(n_R, n_T)$.

On the other hand, GMD decomposes the channel matrix into

$$\mathbf{H} = \mathbf{Q} \cdot \mathbf{\Sigma} \cdot \mathbf{P}^H , \quad (4)$$

where the $(n_R \times n_R)$ matrix \mathbf{Q} and the $(n_T \times n_T)$ matrix \mathbf{P} are composed of orthogonal columns, and $\mathbf{\Sigma}$ is a real upper triangular matrix where the off-diagonal elements represent the remaining interferences and all the elements in the main diagonal take the same value which is the geometric mean of the positive square roots of the eigenvalues of the matrix $\mathbf{H}^H \mathbf{H}$ given by

$$r_{ii} = \left(\prod_{i=1}^L \sqrt{\xi^{(i)}} \right)^{1/L} , \quad (5)$$

where the parameters $\sqrt{\xi^{(i)}} > 0$ (for $i = 1, 2, \dots, L$) are the singular values of \mathbf{H} and L defines the number of activated MIMO layers.

When applying the proposed GMD scheme, the MIMO system requires appropriate pre- and post-processing in order to decompose the MIMO system into multiple SISO channels and the transmission system results in

$$\mathbf{y} = \mathbf{Q}^H \cdot \mathbf{u} = \mathbf{Q}^H (\mathbf{H} \cdot \mathbf{c} + \mathbf{n}) = \mathbf{Q}^H (\mathbf{H} \cdot \mathbf{P} \cdot \mathbf{x} + \mathbf{n}) , \quad (6)$$

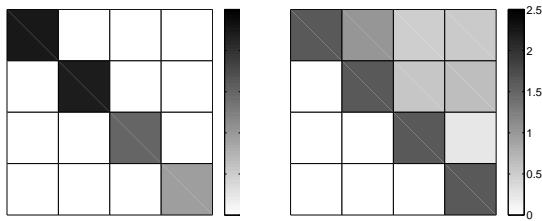


Figure 1: Graphical representation of the matrix \mathbf{V} (left) and the matrix Σ (right).

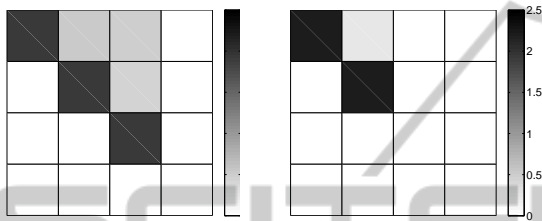


Figure 2: Graphical representation of the matrix Σ with $L = 3$ (left) and $L = 2$ activated layers (right).

and can be represented as

$$\mathbf{y} = \Sigma \cdot \mathbf{x} + \mathbf{w} \quad (7)$$

where \mathbf{x} is the $(n_T \times 1)$ pre-processed transmit data vector, \mathbf{y} is the $(n_R \times 1)$ post-processed data vector at the receiver side and $\mathbf{w} = \mathbf{Q}^H \cdot \mathbf{n}$ is the $(n_R \times 1)$ post-processed noise vector.

The required signal processing in both SVD- and GMD-based MIMO transmission systems modifies neither the transmit power nor the noise levels since the pre- and post-processing matrices are unitary.

Fig. 1 compares the distribution of the singular values of the matrix \mathbf{V} and the geometric mean of the singular values of the matrix Σ . The analysis of Fig. 1 highlights the unequal weighting in the SVD-based MIMO system (left) and the equal weighting as well as the remaining inter-antennas interferences in the GMD-based MIMO system (right). Fig. 2 shows a representation of the matrix Σ for a different number of activated layers.

The proximity between the antennas introduces correlation effect which drops the MIMO system performance. Transmit-side antennas correlation describes the similitude between the paths corresponding to a pair of antennas (at the transmitter side) with respect to a reference antenna (at the receiver side). The antennas' correlation affects the singular values distribution and increases the probability of having predominant layers. The appearance of predominant weak and strong layers with small and large singular values respectively increases the BER.

To analyse the correlation effect, the ratio ϑ

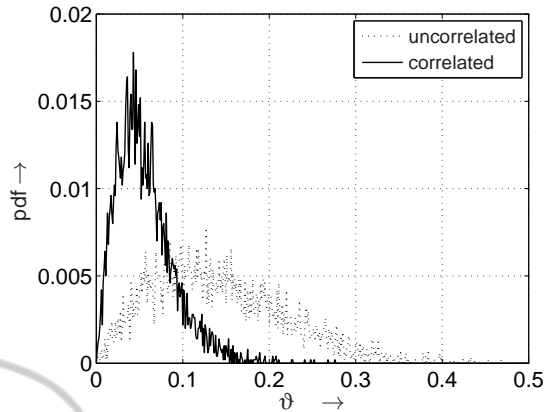


Figure 3: PDF of the ratio ϑ between the smallest and the largest singular value for uncorrelated (dotted line) as well as correlated (solid line) frequency non-selective (4×4) MIMO channel.

between the smallest and the largest singular values seems to be a unique indicator of the unequal weighting of the MIMO layers. Fig. 3 shows the probability density function (PDF) of the ϑ for uncorrelated and correlated frequency non-selective (4×4) MIMO systems. Fig. 3 illustrates how the ratio between the singular values increases (i.e the unequal weighting) as the correlation does. This means that the ratio between the largest and the smallest singular value increases, and then, the probability of having predominant layers increases. In consequence, the probability of having weak layers with layer poor behaviour increases and transmit-to-receive antenna paths become similar affecting the channel behaviour by decreasing the channel capacity and increasing the overall BER in the wireless communication link. As a result, the use of resource allocation techniques seems an appropriate solution to optimize the layer behaviour since no power should be allocated to the MIMO layer having the smallest singular values because of the overall performance would be deteriorated.

Fig. 4 shows a comparison between the PDF of the geometric mean of the singular values of the matrix Σ for uncorrelated and correlated (4×4) MIMO systems. The analysis of the PDF reveals the decreasing probability of having larger values of the geometric mean in the correlated GMD-based MIMO systems compared to the uncorrelated ones. As an example, analysing the PDF curves for a fixed $\vartheta = 2$, the probability of the geometric mean of the singular values in the uncorrelated GMD-based MIMO channel takes 10 times (approximately) larger than in the correlated one. This means that increasing the correlation, the probability of having larger values decreases and con-

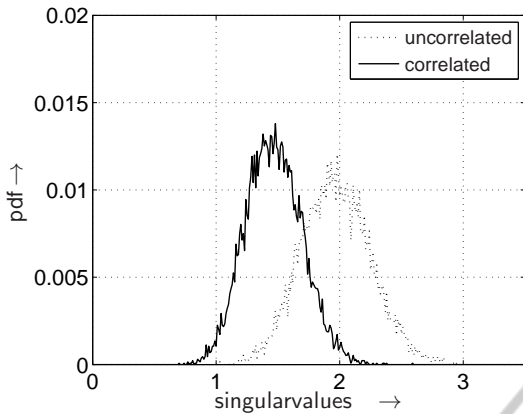


Figure 4: PDF of the geometric mean of the singular values of the matrix Σ without correlation (dotted line) and with correlation (solid line) when using $L = 3$ activated layers.

sequently, the MIMO performance drops. Further comparisons between the BER performance of the SVD-based and the GMD-based MIMO systems are accomplished in following sections.

3 QUALITY CRITERIA

The quality criteria considered for end-to-end wireless communication system performance is given in terms of the bit-error-rate (BER), which quantifies the reliability of the entire wireless system from input to output.

In order to optimize the overall channel performance the argument of the complementary error function, also known as signal-to-noise ratio (SNR), is maximized as an alternative to minimizing the BER. The SNR per quadrature component is defined by

$$\rho = \frac{(U_A)^2}{(U_R)^2}, \quad (8)$$

where U_A is the half vertical eye opening and U_R^2 is the noise power per quadrature component taken at the detector input. The relationship between the signal-to-noise ratio ρ and the bit-error probability evaluated for AWGN channels and M -ary Quadrature Amplitude Modulation (QAM) is given by

$$P_b = \frac{2}{\log_2(M)} \cdot \left(1 - \frac{1}{\sqrt{M}}\right) \cdot \text{erfc} \left(\sqrt{\frac{\rho}{2}} \right). \quad (9)$$

The application of the SVD pre- and post-processing leads to an unequally weighted SISO channel (see Fig. 5) with different eye openings per activated MIMO layer ℓ and per transmitted symbol block k according to

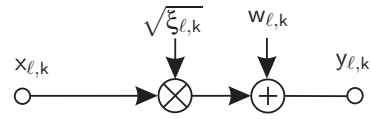


Figure 5: System model per MIMO layer ℓ and transmitted data block k after SVD pre- and post-processing.

$$U_A^{(\ell,k)} = \sqrt{\xi_{\ell,k}} \cdot U_{s\ell}, \quad (10)$$

where $U_{s\ell}$ denotes the half-level transmit amplitude assuming M_ℓ -ary QAM and $\sqrt{\xi_{\ell,k}}$ represents the positive square roots of the eigenvalues of the matrix $\mathbf{H}^H \mathbf{H}$. Considering QAM constellations, the average transmit power per MIMO layer $P_{s\ell}$ may be expressed as

$$P_{s\ell} = \frac{2}{3} U_{s\ell}^2 (M_\ell - 1). \quad (11)$$

By taking $L \leq \min(n_T, n_R)$ MIMO activated layers into account, the overall transmit power results in

$$P_s = \sum_{\ell=1}^L P_{s\ell}. \quad (12)$$

where P_s is the total available power at the transmit side. The layer-specific bit-error probability at the time slot k is obtained by combining (8), (9), and (10) resulting in

$$P_b^{(\ell,k)} = \frac{2}{\log_2(M_\ell)} \left(1 - \frac{1}{\sqrt{M_\ell}}\right) \text{erfc} \left(\frac{U_A^{(\ell,k)}}{\sqrt{2} U_R} \right). \quad (13)$$

The aggregate bit-error probability at the time slot k , taking L activated MIMO-layers into account, results in

$$P_b^{(k)} = \frac{1}{\sum_{v=1}^L \log_2(M_v)} \sum_{\ell=1}^L \log_2(M_\ell) P_b^{(\ell,k)}. \quad (14)$$

Finally, the BER of the whole MIMO system is obtained by considering the different transmission block SNRs. In order to balance the bit error probability along the MIMO system activated layers, bit and power loading provides helpful strategies to improve the overall performance. The bit error probability at a given time k is influenced by both the chosen QAM constellation and the layer-specific weighting factors. In particular, the layer-specific weighting factors influence the overall performance.

Table 1: Investigated QAM transmission modes assuming $n_R = n_T = 4$.

throughput	layer 1	layer 2	layer 3	layer 4
8 bit/s/Hz	256	0	0	0
8 bit/s/Hz	64	4	0	0
8 bit/s/Hz	16	16	0	0
8 bit/s/Hz	16	4	4	0
8 bit/s/Hz	4	4	4	4

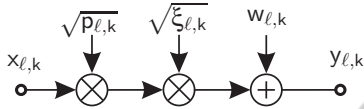


Figure 6: Resulting layer-specific system model including MIMO-layer PA.

4 RESOURCE ALLOCATION

Resource allocation strategies allow the optimization of the MIMO channel overall performance. Hence, the BER can be minimized under the constraints of a fixed data rate and a limited available transmit power. Regarding the channel quality, the BER performance is affected by both the layer-specific weighting factors $\sqrt{\xi_{l,k}}$ and the QAM-constellation size M_ℓ . Assuming a fixed data rate, regardless of the channel quality, Table 1 highlights the resulting layer-specific QAM constellations for a fixed spectral efficiency of 8 bit/s/Hz. Following the allocation of bits per layer, power allocation (PA) can be added to optimize the overall BER. The layer-specific power allocation weights $\sqrt{p_{l,k}}$ adjust the half-vertical eye opening per symbol block as follows (see Fig. 6)

$$U_{\text{APA}}^{(\ell,k)} = \sqrt{p_{l,k}} \cdot \sqrt{\xi_{l,k}} \cdot U_{s\ell} . \quad (15)$$

This results in the layer-specific transmit power per symbol block k

$$P_{s\text{ PA}}^{(\ell,k)} = p_{l,k} \cdot P_{s\ell} , \quad (16)$$

where $P_{s\ell}$ denotes the allocated power per MIMO layer without PA e. g. $P_{s\ell} = P_s/L$. Therein the parameter L describes the number of activated MIMO layers. Taking all activated MIMO layers L into account, being $L \leq \min(n_T, n_R)$, the overall transmit power per symbol block k is obtained as

$$P_{s\text{ PA}}^{(k)} = \sum_{\ell=1}^L P_{s\text{ PA}}^{(\ell,k)} . \quad (17)$$

With (15) the layer-specific bit-error probability at the time k changed to

Table 2: Investigated channel profiles for studying the effect of optimum power allocation.

Profile	layer 1	layer 2	layer 3	layer 4
CM-1	1,7500	0,8750	0,4375	0,2188
CM-2	1,9000	0,6333	0,2111	0,0704

$$P_{\text{bPA}}^{(\ell,k)} = \frac{2}{\log_2(M_\ell)} \left(1 - \frac{1}{\sqrt{M_\ell}}\right) \operatorname{erfc} \left(\frac{U_{\text{APA}}^{(\ell,k)}}{\sqrt{2}U_R} \right) . \quad (18)$$

In order to find the optimal set of PA parameters minimizing the overall BER, i. e., $\sqrt{p_{l,k}}$, the Lagrange multiplier method is used. The cost function for this method $J(p_{1,k}, p_{2,k}, \dots, p_{L,k})$ may be expressed as

$$J(\dots) = \frac{1}{\sum_{v=1}^L \log_2(M_v)} \sum_{\ell=1}^L \log_2(M_\ell) P_{\text{b}}^{(\ell,k)} + \lambda \cdot B , \quad (19)$$

where λ denotes the Lagrange multiplier. The parameter B in (19) describes the boundary condition to meet the overall transmit power constraints

$$B = \sum_{\ell=1}^L (P_{s\ell} - P_{s\text{ PA}}^{(\ell,k)}) = 0 \quad (20)$$

$$= \sum_{\ell=1}^L P_{s\ell} (1 - p_{l,k}) = 0 . \quad (21)$$

Assuming $P_{s\ell} = P_s/L$, the boundary condition results in

$$B = \frac{P_s}{L} \sum_{\ell=1}^L (1 - p_{l,k}) = 0 . \quad (22)$$

Given (22), the transmit power coefficients have to fulfill the following equation $\sum_{\ell=1}^L p_{l,k} = L$. Differentiating the Lagrangian cost function $J(p_{1,k}, p_{2,k}, \dots, p_{L,k})$ with respect to the $p_{l,k}$ and setting it to zero, leads to the optimal set of PA parameters.

In order to analyse the effect of PA thoroughly, the fixed channel profiles shown in Table 2 are investigated. For comparison reasons, the channel profile CM-1 describes a MIMO channel with a low degree of correlation ($\vartheta = 0,125$) whereas the channel CM-2 introduces a higher degree of antennas' correlation ($\vartheta = 0,037$). In this case the unequal weighting of the layers becomes stronger compared to the channel profile CM-1.

Since the optimal PA solution is notably computationally complex to implement, a suboptimal solution

which concentrates on the argument of the complementary error function is investigated. In this particular case the signal-to-noise ratio

$$\rho_{\text{PA}}^{(\ell,k)} = \frac{\left(U_{\text{A PA}}^{(\ell,k)}\right)^2}{U_{\text{R}}^2} \quad (23)$$

is assumed to be equal for all activated MIMO layers per data block k , i.e., $\rho_{\text{PA}}^{(\ell,k)} = \text{constant}$ $\ell = 1, 2, \dots, L$.

Assuming that the transmit power coefficient per layer is uniformly distributed, the power to be allocated to each activated MIMO layer ℓ and transmitted data block k can be simplified as follows:

$$p_{\ell,k} = \frac{(M_{\ell} - 1)}{\xi_{\ell,k}} \cdot \frac{L}{\sum_{v=1}^L \frac{(M_v - 1)}{\xi_{v,k}}} \quad (24)$$

Hence, for each symbol the same half vertical eye opening of (15) can be guaranteed ($\ell = 1, \dots, L$), i.e.,

$$U_{\text{A PA}}^{(\ell,k)} = \text{constant} \quad \ell = 1, 2, \dots, L \quad (25)$$

Considering an identical noise power at the detector's input, the above-mentioned equal quality scenario is encountered.

The BER curves for channel profiles CM-1 and CM-2 are shown in Fig. 7 and Fig. 8. In order to use the MIMO channel in an optimized way not all the MIMO layers should be necessarily activated. Furthermore, PA in combination with an appropriate selection of number of activated MIMO layers guarantees the best BER performance when transmitting at a fixed data rate of with spectral efficiency 8 bit/s/Hz.

In Fig. 9 the obtained BER curves with the optimal PA based on the Lagrange multiplier method are shown considering the above mentioned equal quality criteria. As demonstrated by computer simulations the loss in the overall BER with the equal quality criteria is quite acceptable when using the optimized bit loading.

Table 3 compares the memory usage and CPU time required to execute the optimal and suboptimal solutions with a processor AMD A4 – 5300 APU at 3.40GHz. It turned out that the proposed suboptimal equal-SNR PA technique presents a lower complexity and computational load than the optimal one.

Fig. 10 shows a comparison of the BER curves among the QAM transmission modes listed in Table 1 with and without PA when transmitting 8 bit/s/Hz over uncorrelated frequency non-selective MIMO channels. It can be seen that not all MIMO layers should be activated in correlated as well as in uncorrelated MIMO channels to minimize the overall BER while transmitting at a fixed data rate.

Table 3: Investigated PA methods for comparing the computational load assuming a (4×4) MIMO system at $10 \log_{10}(E_s/N_0) = 20$ dB.

Power Allocation	Memory	Time
Optimal	9.80 MiB	200.00 ms
Suboptimal	0.22 MiB	5.00 ms

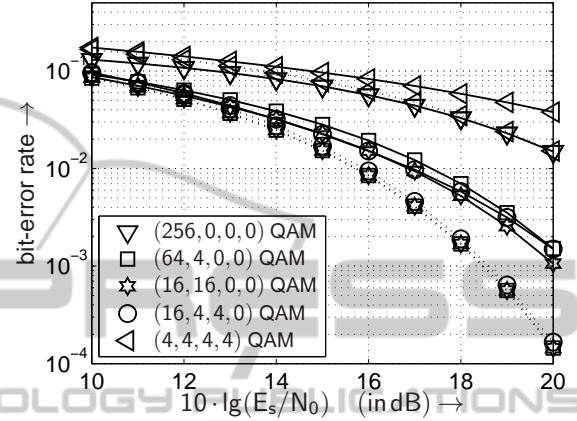


Figure 7: BER with optimal PA (dotted line) and without PA (solid line) when using the transmission modes introduced in Table 1 and transmitting 8 bit/s/Hz over channel CM-1.

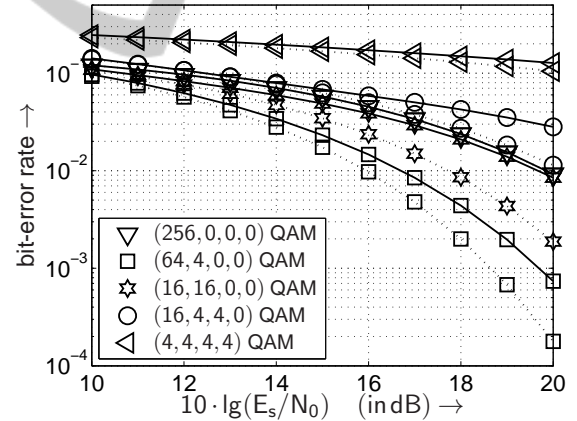


Figure 8: BER with optimal PA (dotted line) and without PA (solid line) when using the transmission modes introduced in Table 1 and transmitting 8 bit/s/Hz over channel CM-2.

5 RESULTS

In this section the computer simulation results concerning the analysis of the SVD-based and the GMD-based MIMO systems are shown. These results highlight the bit- and power-allocation strategies which obtain the best performance. Furthermore, the best results are compared when using the SVD-based and GMD-based systems.

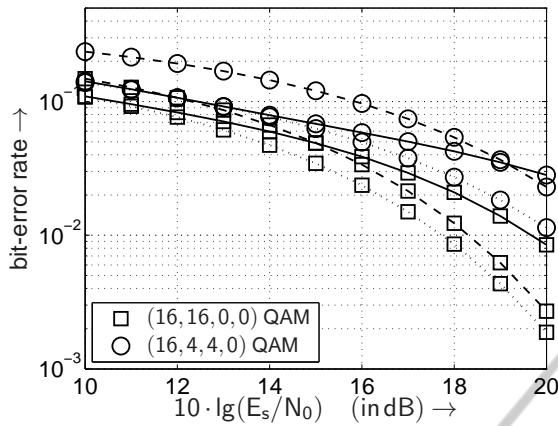


Figure 9: BER with optimal PA (dotted line), equal-SNR PA (dashed line) and without PA (solid line) when using the transmission modes introduced in Table 1 and transmitting 8 bit/s/Hz over channel CM-2.

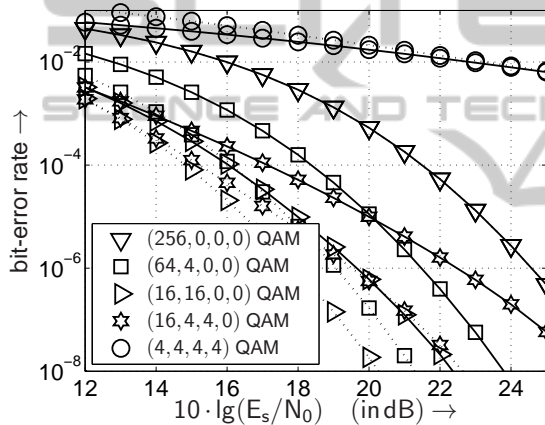


Figure 10: BER with PA (dotted line) and without PA (solid line) when using the transmission modes introduced in Table 1 and transmitting 8 bit/s/Hz over uncorrelated frequency non-selective MIMO channels.

The accomplished results show how the selection of the most favourable QAM transmission mode, the optimal transmit power allocation per active layer and time slot as well as the proper mathematical decomposition achieves the best BER performance.

Fig. 11 shows the BER curves of the SVD-based MIMO system and remarks the poor performance obtained in the presence of correlation. When transmitting the same QAM constellation through the best two layers, the channel affected by antennas' correlation performs much worse than the uncorrelated. On the other hand, when transmitting unequal QAM constellations through the two activated layers, the channel affected by antennas correlation performs worse than the uncorrelated, but the performance difference is not as notably as the case with equal QAM constellations. This means that bit-allocation is specially

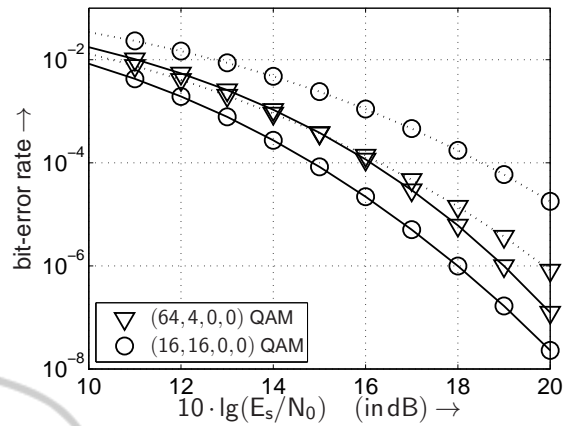


Figure 11: BER performance with SVD processing and equal-SNR PA when using the transmission modes introduced in Table 1 and transmitting 8 bit/s/Hz over frequency non-selective (4×4) MIMO channels without correlation (solid line) and with correlation (dotted line).

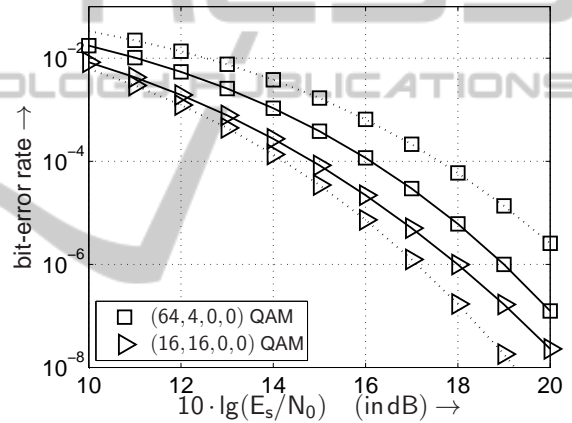


Figure 12: BER curves with GMD processing (dotted line) assuming perfect interference cancellation compared to BER curves with SVD (solid line) when using the transmission modes introduced in the legend with equal-SNR PA and transmitting 8 bit/s/Hz over frequency non-selective (4×4) MIMO channels without antenna correlation.

useful in MIMO channels affected by antennas' correlation. Fig. 12 shows the BER performance of the GMD-based (4×4) MIMO system (assuming perfect remaining interference cancellation) compared to the SVD-based (4×4) MIMO system, both for frequency non-selective channels. Fig. 13 extends that analysis to the case in which the channels are affected by antennas correlation. The analysis of Fig. 12 highlights that when unequal QAM modes are used on the two activated layers (consider the transmission mode analysed), the SVD-based system presents a superior performance than the GMD-based. This is due to the unequal performance of the two layers in the SVD-based MIMO system.

On the other hand, when transmitting equal QAM

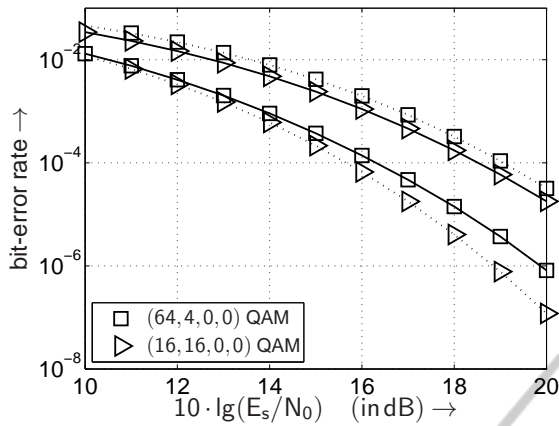


Figure 13: BER curves with GMD technique (dotted line) assuming perfect interference cancellation compared to BER curves with SVD (solid line) when using the transmission modes introduced in the legend with equal-SNR PA and transmitting 8 bit/s/Hz over frequency non-selective (4×4) MIMO channels with antenna correlation.

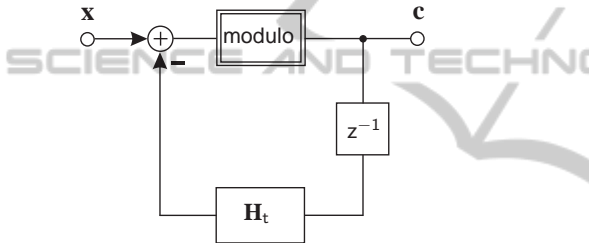


Figure 14: Tomlinson-Harashima precoding model in the transmission side for MIMO systems.

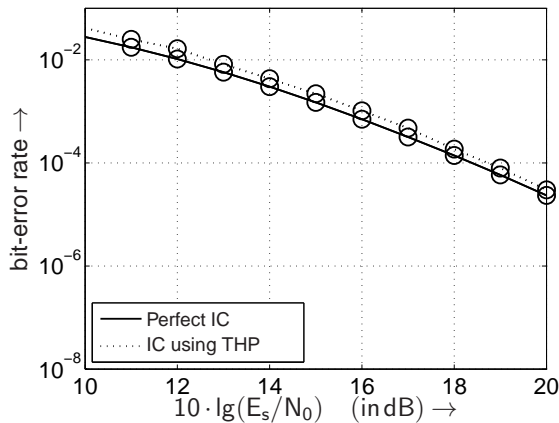


Figure 15: BER comparison between Perfect Interference Cancellation and Interference Cancellation using THP when using the transmission mode (4,4,4,4) and transmitting 8 bit/s/Hz over uncorrelated frequency non-selective GMD-based MIMO channels.

modes through the two activated layers, the GMD-based MIMO system shows the best results, as both layers present the same performance. These conclusions are reinforced by the results in Fig. 13 for cor-

related channels. In this case, as the performance of the two activated layers is much more different in the SVD-based MIMO system, the use of unequal QAM modes along the activated layers becomes more important to obtain a better performance. In this case the SVD-based system shows a superior performance than the GMD-based. Nevertheless, the results highlight that the use of equal QAM modes along the activated layers is much more appropriate for the GMD-based MIMO system. Then, GMD-based MIMO systems do not require bit allocation strategies to obtain the best performance. Nevertheless, SVD-based systems require bit allocation to improve the channel performance.

In order to eliminate the inter-antennas interference and the error propagation in the GMD-based MIMO systems a Tomlinson-Harashima precoding (THP) module is proposed at the transmitted side. Fig. 14 shows the THP system model where \mathbf{x} corresponds to the ($n_T \times 1$) transmitted vector followed by a modulo reduction which suppresses the power enhancement. Assuming perfect channel state information is available at the transmitter side, \mathbf{H}_t is given by

$$\mathbf{H}_t = \mathbf{\Sigma} - \text{diag}(\mathbf{\Sigma}) \cdot \mathbf{I}, \quad (26)$$

where $\mathbf{\Sigma}$ corresponds with a real upper triangular matrix, $\text{diag}(\cdot)$ are the main diagonal elements and \mathbf{I} is the identity matrix. The modulo operator (Fig. 14) constraints the real and imaginary part of the transmit symbols into the boundary constellation of width of the modulo operator. This modulo is defined by $\text{modulo}(\Delta \cdot q) = \text{modulo}(2 \cdot U_s \cdot q)$, where Δ is the distance between two adjacent symbols, U_s denotes the half-level transmit amplitude and $q = \sqrt{M}$, being M the modulation index in every active MIMO layer.

In Fig. 15 a comparison between perfect interference cancellation technique and THP interference cancellation for a (4,4,4,4) QAM transmission mode is shown. The results reveal that the GMD-based MIMO system performance with THP is close to those obtained when perfect interference cancellation is assumed. The losses are about 0.5 dB compared to the perfect cancellation. In consequence the THP seems to be an appropriate strategy to eliminate the GMD-based system remaining interference with little computational complexity overhead.

6 CONCLUSION

This paper has investigated the use of bit- and power-allocation techniques to improve the performance of SVD-based as well as GMD-based MIMO systems

as demonstrated by the performed analysis and the shown results. The combination of these techniques remarkably improves the channel performance, even when suboptimal algorithms are used where little losses are produced. Nevertheless, these techniques include some processing overhead which can be reduced by using suboptimal solution with low performance losses.

A relevant challenge and achievement of this investigation is the introduction of the GMD signal processing to improve the MIMO channel performance. The analysis focusses on both uncorrelated and correlated (4×4) MIMO channels and the results are compared with those obtained when using the SVD signal processing, combined with bit- and power-allocation techniques.

GMD-based MIMO systems show remaining inter-antennas interferences. Hence, some additional signal processing techniques must be applied to remove it. The THP has demonstrated to be an appropriate technique to remove the interferences with low losses compared to the perfect interference elimination case.

According to the obtained results the combination of GMD-based MIMO systems with the THP shows a noteworthy BER performance improvement compared to the SVD-based MIMO system. First, assuming the remaining inter-antennas interferences have been completely removed, the GMD-based MIMO system shows equal quality SISO channels (layers) and, in consequence, bit- and power-allocation techniques are not required as they do not improve the channel performance. Conversely, the performance drops. This conclusion applies to both antennas uncorrelated and correlated channels. The SVD-based MIMO channel requires the application of bit- and power-allocation techniques to improve the performance, as it presents unequal quality layers. Second, when bit allocation is applied to both the SVD-based and GMD-based MIMO systems, as shown in our work, the SVD-based one presents a superior performance, because in the GMD-based system the advantage of having equal quality layers is not taken when transmitting data with different QAM constellation sizes. Finally, the obtained results demonstrate that the GMD-based MIMO system with remaining inter-antennas interference cancellation by using the THP shows a superior performance than the SVD-based system without requiring bit- and power-allocation techniques, which notably reduces the computational complexity and overhead.

REFERENCES

- Abdi, A. and Kaveh, M. (2002). A Space-time Correlation Model for Multielement Antenna Systems in Mobile Fading Channels. *IEEE Journal on Selected Areas in Communications*, 20:550–560.
- Benavente-Peces, C., Cano-Broncano, F., Ahrens, A., Ortega-Gonzalez, F., and Pardo, J. (2013). Analysis of Singular Values PDF and CCDF on Receiver-Side Antennas Correlated MIMO Channels. *Electronics Letters*, 49, Issue: 9:625–627.
- Cano-Broncano, F., Ahrens, A., and Benavente-Peces, C. (Lisboa, Portugal), 7-9 January 2014). Iterative Bit- and Power Allocation in Correlated MIMO Systems. In *International Conference on Pervasive and Embedded Computing and Communication Systems (PECCS)*.
- Chiani, M., Win, M., and Zanella, A. (2003). On the Capacity of Spatially Correlated MIMO Rayleigh-Fading Channels. *IEEE Transactions on Information Theory*, 49:2363–2371.
- Jiang, Y., Hager, W., and Jian, L. (2008). The Generalized Triangular Decomposition. *Mathematics of Computation*, 77:1037–1056.
- Jiang, Y., Li, J., and Hager, W. (2005). Joint Transceiver Design for MIMO Communications Using Geometric Mean Decomposition. *IEEE Transactions on Signal Processing*, 53:3791–3803.
- Loyka, S. and Tsoulos, G. (2002). Estimating MIMO System Performance using the Correlation Matrix Approach. *IEEE Communications Letters*, 6:19 – 21.
- Shiu, D.-S., G.J. F., Gans, M., and Kahn, J. (1998). Fading Correlation and its effect on the Capacity of multi-element Antenna Systems. In *Universal Personal Communications*.
- Yang, P., Xiao, Y., Yu, Y., and Li, S. (2011). Adaptive Spatial Modulation for Wireless MIMO Transmission Systems. *IEEE Communications Letters*, 15:602–604.
- Zanella, A. and Chiani, M. (2012). Reduced Complexity Power Allocation Strategies for MIMO Systems with Singular Value Decomposition. *IEEE Transactions on Vehicular Technology*, 61:4031–4041.
- Zheng, L. (2003). Diversity and Multiplexing: A Fundamental Tradeoff in Multiple-Antenna Channels. *IEEE Transactions on Information Theory*, 49:1073–1096.